Available online at www.sciencedirect.com
ScienceDirect
Trans. Nonferrous Met. Soc. China 28(2018) 2419−2426
Transactions of Nonferrous Metals Society of China
www.tnmsc.cn

Enhanced strengthening by two-step progressive solution and aging treatment in AM50−4%(Zn,Y) magnesium alloy

Shuai DAI, Feng WANG, De-zhi MA, Zhi WANG, Zheng LIU, Ping-li MAO

School of Materials Science and Engineering, Shenyang University of Technology, Shenyang 110870, China

Received 21 December 2017; accepted 19 June 2018

Abstract: AM50−4%(Zn,Y) alloy with a Zn/Y mole ratio of 6:1 was subjected to thermal analysis, and the results were used for designing a two-step progressive solution treatment process. The effects of solution and aging treatments on the microstructure and mechanical properties of the AM50−4%(Zn,Y) alloy were investigated using OM, XRD, SEM/EDS, TEM, tensile test and hardness test. The experimental results demonstrated that the two-step progressive solution treatment could make the Φ and β phases sufficiently dissolve into the matrix which possessed higher supersaturated degree of the dissolved solute compared with the one-step solution treatment. This resulted in a certain enhancement of the precipitation strengthening effect during the subsequent aging process. The precipitation of the Φ phase had a greater impact on the comprehensive mechanical properties of the alloy than β phase precipitation when the aging treatment was performed at 180 °C. The peak aging strength of the AM50−4%(Zn,Y) alloy which was subjected to the two-step progressive solution treatment process (345 °C for 16 h and 375 °C for 6 h) was obtained after the aging treatment at 180 °C for 12 h.

Key words: AM50−4%(Zn,Y) alloy; thermal analysis; solution; aging treatment; microstructure; strengthening mechanism

1 Introduction

Recently, the applications of magnesium alloys have been continuously expanded due to their superior mass reduction and advantageous properties [1]. Among the commercial magnesium alloys, Mg−Al system alloys such as AM50, AM60, AZ91 and AZ61 were the first to be developed, and they have also been most widely used in different applications. However, these alloys exhibited unsatisfactory strength and ductility both at room and elevated temperature, due to the coarse morphology and low thermal stability of the β-$Mg_{17}Al_{12}$ phase. Recently, some studies have revealed that the alloying as Ca, Sb, Sr, Si, Sn or RE element addition was an effective method to improve the mechanical properties of the Mg−Al system alloys. This approach improves the properties by refining the grain size, decreasing the amount and improving the morphology of the β phase, while consequently new beneficial phases such as Al_2Ca, Mg_3Sb_2, Al_4Sr, Mg_2Si, Mg_2Sn and Al-RE are formed [2−6]. Furthermore, the new Mg−Zn−Al(ZA) alloys with high Zn content have been attracted widespread attention due to their excellent high temperature resistance, creep resistance and low cost [7]. It has also been reported that the addition of Cu to Mg−Zn−Al alloys could refine the eutectic besides accelerating the age-hardening, thus leading to the obvious improvement of the ambient and elevated temperature strength characteristics [8].

Mg−Zn−Al alloys can be considered to be one of the most promising heat treatable alloy types due to their excellent age-hardening response. Corresponding results have indicated that there is a great potential to further increase the strength via various heat treatments, and the effort has been made to further improve the precipitation strengthening effect of the Mg−Zn−Al series alloys by multi-alloying [9]. It is, however, challenging to get the second phases which are formed during alloying to completely dissolve into the matrix through traditional solution treatments where the treatment temperature is 10−20 °C below the solidus temperature for some magnesium alloys [10]. This limitation can be circumvented by using a longer solution time or higher

Foundation item: Project (201602548) supported by Liaoning Province Natural Science Foundation, China; Project (1711800) supported by Shenyang Science and Technology Plan, China; Project (LQGD2017032) supported by Youth Project of Liaoning Education Department, China; Projects (51504153, 51571145) supported by the National Natural Science Foundation of China

Corresponding author: Feng WANG; Tel: +86-15002424621; Fax: +86-24-25496768; E-mail: wf9709@126.com

DOI: 10.1016/S1003-6326(18)64888-5

solution temperature. This will, however, have a deteriorating effect on the properties of these alloys. Therefore, a two-step solid solution method has been developed and applied in order to make the second phases fully dissolve into the α-Mg matrix of the AZ64 alloy, thus obtaining better subsequent age-strengthening properties [11].

In our previous work related to similar alloys [12], it was not possible to form the quasicrystal *I*-phase (Mg_3Zn_6Y) when using the AM50−(Zn,Y) alloy with an mole ratio of 6:1 for Zn to Y. Nevertheless, the mechanical properties of the alloy were obviously improved. Thus, in this work, the AM50−4%(Zn,Y) alloy with the best comprehensive mechanical property was chosen for further study. The effects of the different heat treatment conditions on the microstructure and mechanical properties of the alloy were investigated.

2 Experimental

2.1 Alloy preparation

The AM50−4%(Zn,Y) alloy was prepared from a commercial AM50 magnesium alloy ingot, high-purity Zn (>99.9%, mass fraction) and Mg−25%Y master alloy. Firstly, the AM50 magnesium alloy was melted at 700 °C in an electric resistance furnace under a protective atmosphere of 99.5% N_2 and 0.5% SF_6 (volume fraction) mixture. The Zn and the Mg−25%Y master alloy were subsequently added into the melts, and the melting temperature was increased to 720 °C. The temperature of 720 °C was maintained for 30 min in order to ensure that the added alloying elements were completely dissolved. Subsequently, the melts were cooled down to 700 °C and poured into a boron nitride (BN) coated metal mold (d70 mm × 130 mm) which had been preheated to a temperature of 200 °C. The actual elemental composition of the sample is presented in Table 1.

Table 1 Elemental composition of sample AM50−4%(Zn,Y) (mass fraction, %)

Al	Mn	Zn	Y	Mg
4.96	0.30	3.38	0.71	Bal.

2.2 Cooling curve

The melted alloy in a graphite crucible was taken out of the electric resistance furnace and a K-type thermocouple (d=1.5mm) with a fine steel tube was immersed into the melts at 700 °C. A schematic of the experimental set-up is presented in Fig. 1. A high-speed data acquisition system that was linked to a computer was utilized to record the cooling data, and the cooling rate was approximately 0.2 °C/s.

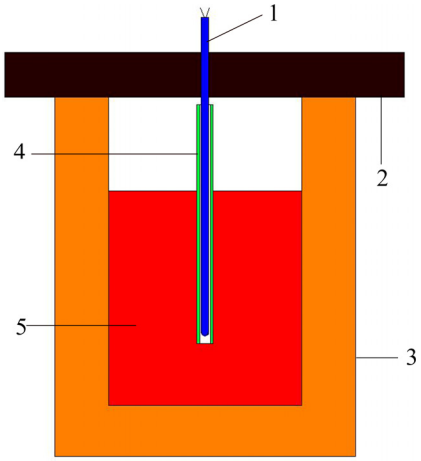

Fig. 1 Test model for determination of solidification curves: 1—K-type thermocouple; 2—Asbestos; 3—Graphite crucible; 4—Steel tube; 5—Liquid metal

2.3 Heat treatment

Based on the thermal analysis result of the AM50−4%(Zn,Y) alloy, the one-step and two-step progressive solution treatments of the alloy were carried out as designed temperature for the required time, then water quenching was adopted. Following, the alloy subjected by one-step and two-step progressive solution treatments with optimum solutionizing parameters were aged at 180 °C for 24 h. For convenience, it could be designated that the two-step progressive solution treatment as $T4_{II}$ and the corresponding T6 treatment as $T6_{II}$, and the others were $T4_I$ and $T6_I$, respectively.

2.4 Microstructure and mechanical properties

The heat treated samples were chemically etched in 4% HNO_3 ethanol solution after mechanical polishing. The microstructure was observed through a Zeiss Axio Observer A1 optical microscope (OM), a Hitachi S−3400N scanning electron microscope (SEM) equipped with an energy dispersive spectroscope (EDS) and a SU8010 field emission scanning electron microscope (FESEM). The phases were analyzed by D/max Ⅲ A X-ray diffraction (XRD) and JEM−2100 transmission electron microscope (TEM). An electric spark machine was utilized to obtain tensile samples from the ingot. The tensile properties were tested using a WDW−100 materials test machine at a stretching speed of 3 mm/min. The hardness was tested using a HVS−5 Vickers indentation test machine. It is worth nothing that the hardness of each sample was obtained from the hardness measurements of six points.

3 Results and discussion

3.1 As-cast microstructure

The SEM image and XRD pattern of the as-cast

alloy are shown in Fig. 2, where the discontinuous strip and granular gray phases are clearly observable. The lamellar eutectics, bright granular intermetallics, as well as fine particles are distributed in the as-cast microstructure. According to the results of the EDS analysis, the compositions of the gray phase and the lamellar eutectic were $Mg_{65.81}Al_{19.52}Zn_{14.67}$ and $Mg_{60.18}Al_{8.39}Zn_{31.43}$, respectively. Combined with the results of XRD, these gray phases were identified as a β-$Mg_{17}(Zn,Al)_{12}$ phase, and the bright lamellar eutectics around the β-$Mg_{17}(Zn,Al)_{12}$ phase were regarded as a Φ-$Mg_{21}(Zn,Al)_{17}$ phase. In addition, it should be noted that the phase containing Y and Mn was not detected by XRD. The bright granular intermetallics were further examined using EDS analysis, the results of which show that the observed Al/Y/Mn mole ratio (33.98:6.12:35.45) was close to 6:1:6 which has been previously identified as the Al_6YMn_6 phase [13]. On the other hand, the excessive Mg content in the spectrum could be attributed to the contribution of the excess Mg within the α-Mg solid solution matrix [14]. The SEM image and elemental maps of the alloy are shown in Fig. 3. The

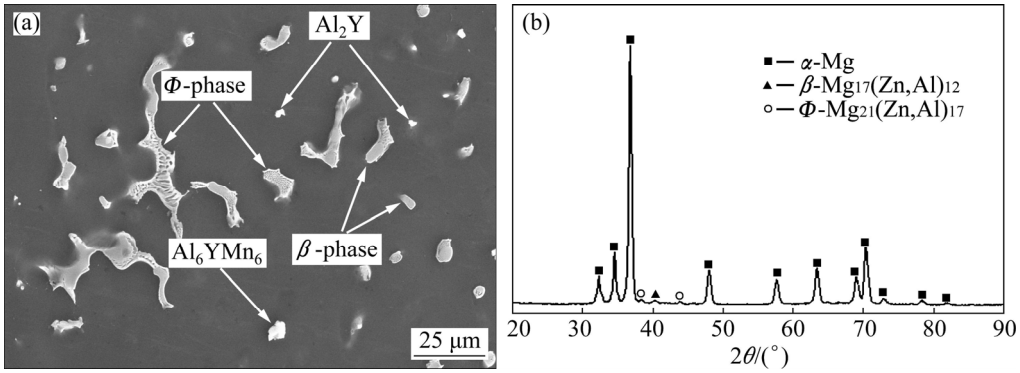

Fig. 2 SEM image (a) and XRD pattern (b) of as-cast alloy

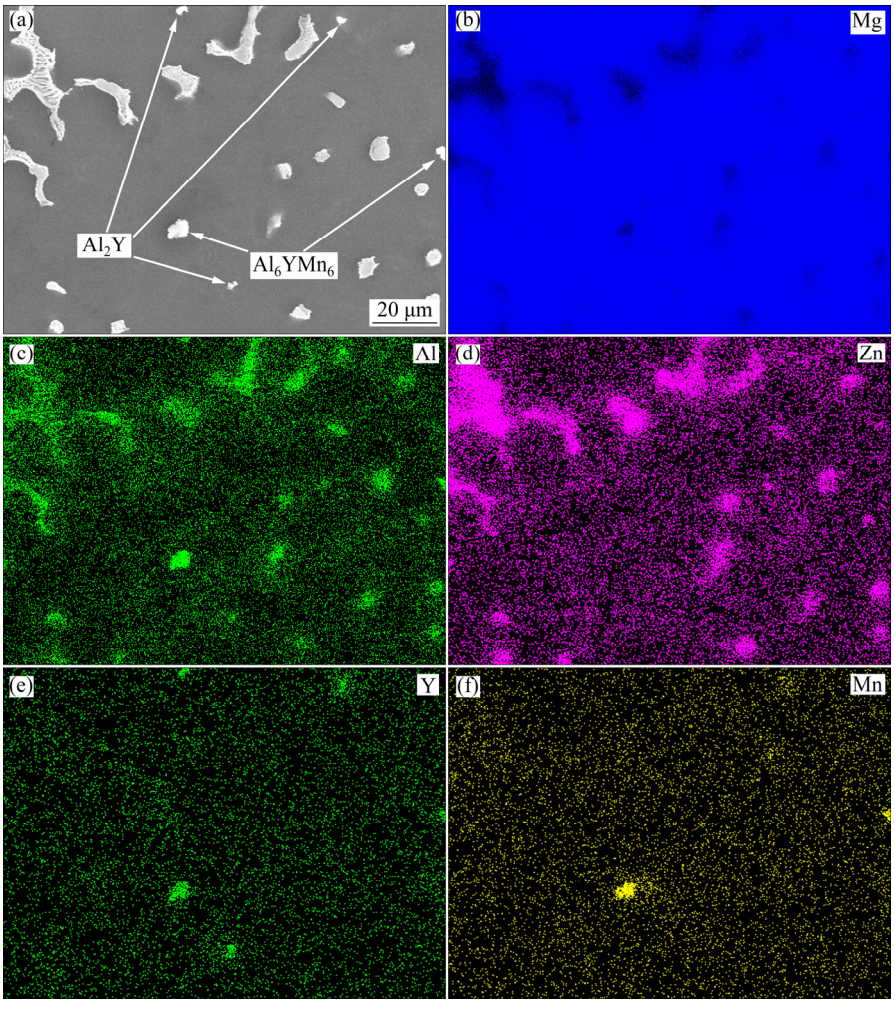

Fig. 3 SEM image (a) and area scan maps of elements Mg (b), Al (c), Zn (d), Y (e) and Mn (f) of as-cast alloy

bright granular intermetallics were enriched with Al, Y and Mn elements, which could be actually further identified as the Al_6YMn_6 phase. Moreover, fine particle Al_2Y phase was also observed in the microstructure and its size was about 1−2 μm due to a pot of Al_6YMn_6, and the Al_2Y phases were resulted from the bare of Y and Mn elements in the alloy, so they were not detected in the XRD pattern.

3.2 Thermal analysis

Thermal analysis is a method to analyze the phase transition by means of using the cooling curve and first derivative curve of cooling curve. The peaks of the first derivative curve can be used to determine the phase transition point of the alloy during solidification [15]. Figure 4 shows three sharp peaks in the first derivative curve, which are related to the solidification process of the alloy and the associated phase transitions. The three peaks are denoted as peak A, peak B and peak C. The reaction temperatures of peak A and peak B are 604.1 °C and 382.3 °C, respectively. These correspond to reactions: $L\rightarrow\alpha$-Mg (peak A) and $L\rightarrow\alpha$-Mg+β (peak B). However, compared with the actual phase transition temperature of 437 °C, the formation temperature of the β phase was low, which is due to the addition of Zn and Y elements [16,17]. Similarly, the peak C could be identified as the Φ phase and the reaction temperature was 353.8 °C which corresponds to the temperature (366 °C) of the peritectic reaction: $L+\beta\rightarrow\Phi+\alpha$-Mg [18]. Based on the results of the thermal analysis, 345 °C was chosen as the one-step solution treatment temperature to ensure that the Φ phase fully dissolved into the α-Mg matrix, and to prevent microstructural over-heating defects. The second solution treatment would be carried out subsequently based on the optimal results of the one-step solid solution treatment. The condition of the second treatment step was chosen so that no Φ phase existed in the microstructure after the first treatment. Therefore, 375 °C was chosen as the second solution treatment temperature to ensure that the β phase fully dissolved into the α-Mg matrix and obtained a significant possible dissolution degree.

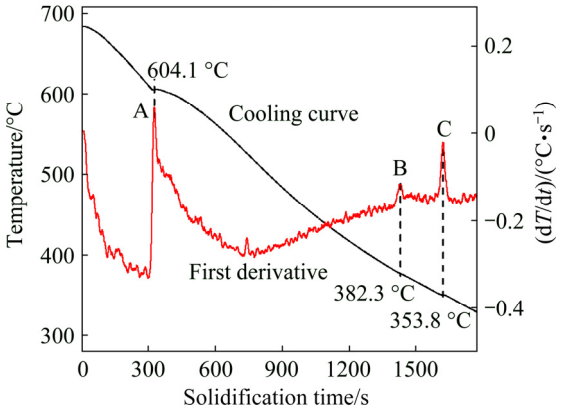

Fig. 4 Thermal analysis result of as-cast alloy

3.3 Solutionizing microstructure

The optical microstructures of the alloys which were obtained after different treatment time using one-step solution treatment at 345 °C are presented in Fig. 5. As shown in Fig. 5, the lamellar Φ-$Mg_{21}(Zn,Al)_{17}$

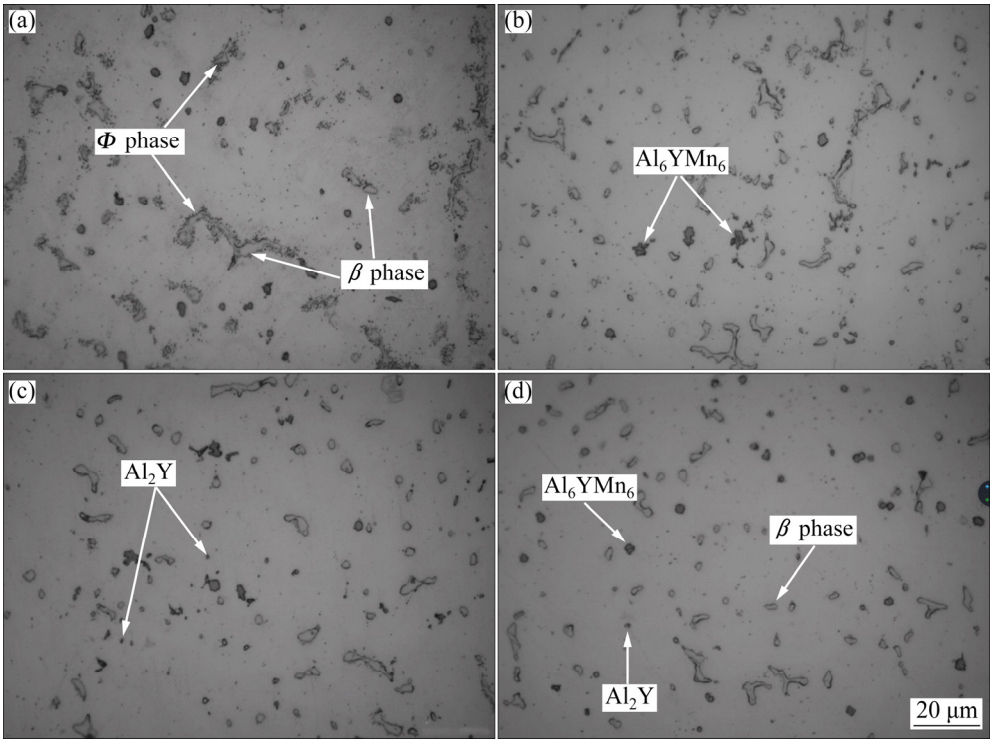

Fig. 5 Microstructures of AM50−4%(Zn,Y) alloy treated at 345 °C for different time ($T4_l$): (a) 4 h; (b) 8 h;(c) 12 h; (d) 16 h

phases around the β-$Mg_{17}(Zn,Al)_{12}$ phases were gradually dissolved into the α-Mg matrix, and the discontinuous strip second phases were transformed into rod-like shapes as the solution time increased. However, the granular Al_6YMn_6 and Al_2Y phases were still distributed in the microstructure due to their excellent thermal stability.

Two-step solution treatment of the alloy at 375 °C with different time was carried out after the (345 °C, 16 h) solution treatment. The microstructures of the alloys which were treated at 375 °C for different time ($T4_{II}$) are presented in Fig. 6. Besides the small quantity of Al_6YMn_6 and Al_2Y phases, all the β-$Mg_{17}(Zn,Al)_{12}$ phases had been dissolved into the α-Mg matrix when the solution time treated at 375 °C was 6 h. Thus, a high degree of dissolution had been obtained.

3.4 Aging microstructure and hardness

Figure 7 shows the SEM images of alloys aged at 180 °C for different time after $T4_I$ and $T4_{II}$ heat treatment. Obviously, the $T6_I$ heat treatment did not cause the β phase to completely dissolve into the α-Mg matrix. Most of fine precipitates were distributed at the grain boundary and interior grain, as shown in Figs. 7(a) and (b). More precipitates could be formed and dispersed uniformly throughout the matrix of the $T6_{II}$ heat-treated alloy, as presented in Figs. 7(c) and (d). For the $T6_I$ and $T6_{II}$ heat-treated alloys, the volume and amount of precipitates increased significantly, and the precipitates around the grain boundaries began to segregate and coarsen when the aging exceeded the optimum condition, as shown in Figs. 7(b) and (d). The TEM observations of the peak-aged alloy ($T6_{II}$ treatment for 12 h) were utilized to further analyze the composition of the fine precipitates after the aging treatment, as shown in Fig. 8. The results show that a mass of nano-scale β phases with the size of 2−4 nm were precipitated from the matrix. Furthermore, some polygonal compounds with the size of 100−200 nm were found in the alloy. These compounds correspond to be the Φ phase. The phase compositions of the AZ64 alloy still contained the β phase and the Φ phase after T6 treatments, which were developed by DONG et al [9] and LIANG et al [11].

The variations of the Vickers hardness of the $T6_I$ and $T6_{II}$ heat-treated alloys with time are presented in Fig. 9. The first point of the curves corresponds to the hardness in the as-cast state. It can be seen that the hardness values for the $T6_I$ and $T6_{II}$ heat-treated alloys first increased, and then subsequently decreased with increasing aging time. In fact, the $T6_I$ and $T6_{II}$ heat-treated alloys obtained their peak hardness values of HV 75 and HV 79 after 12 h. The hardness of the alloy that was prepared by the T6 treatment could be controlled by the amount and the morphology of the precipitation phases. Interestingly, the peak hardness value of the $T6_{II}$ heat-treated alloy was higher than that of the $T6_I$ heat-treated alloy, which clearly indicated that the precipitation of the Φ phase had a greater impact on the hardness of the alloy than the β phase.

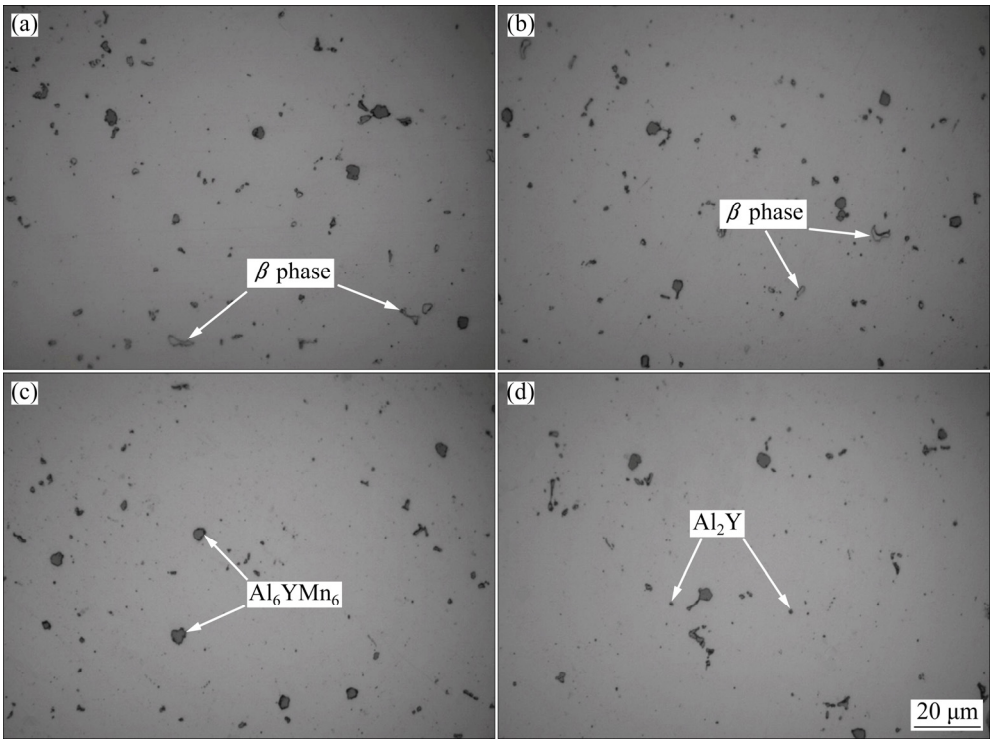

Fig. 6 Microstructures of AM50−4%(Zn,Y) alloy treated at 375 °C for different time ($T4_{II}$): (a) 2 h; (b) 4 h; (c) 6 h; (d) 8 h

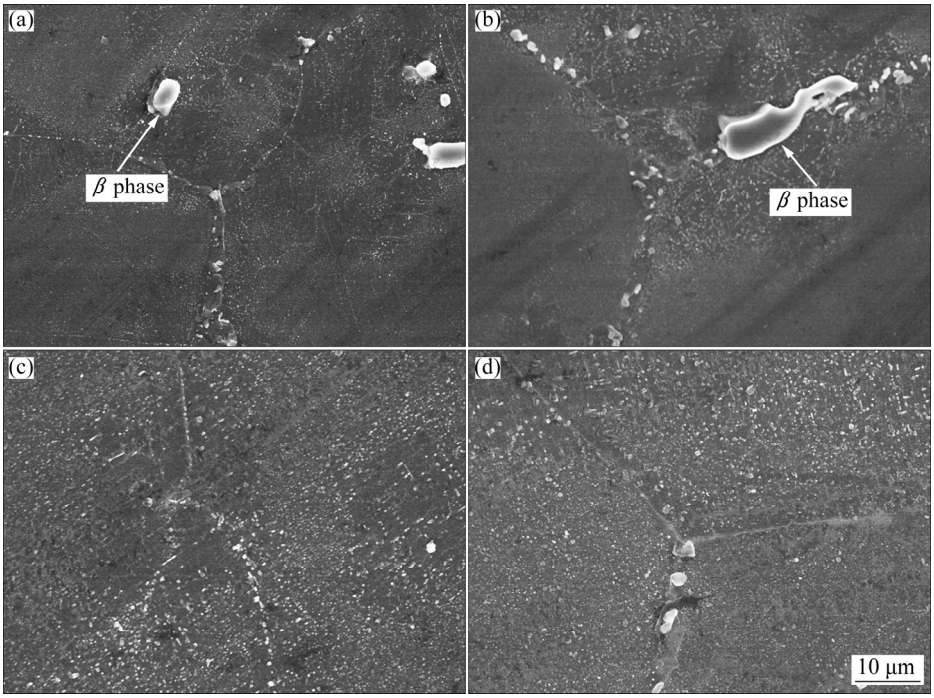

Fig. 7 SEM images of AM50−4%(Zn,Y) alloy treated at 180 °C for different time: (a) $T6_I$, 12 h; (b) $T6_I$, 18 h; (c) $T6_{II}$, 12 h; (d) $T6_{II}$, 18 h

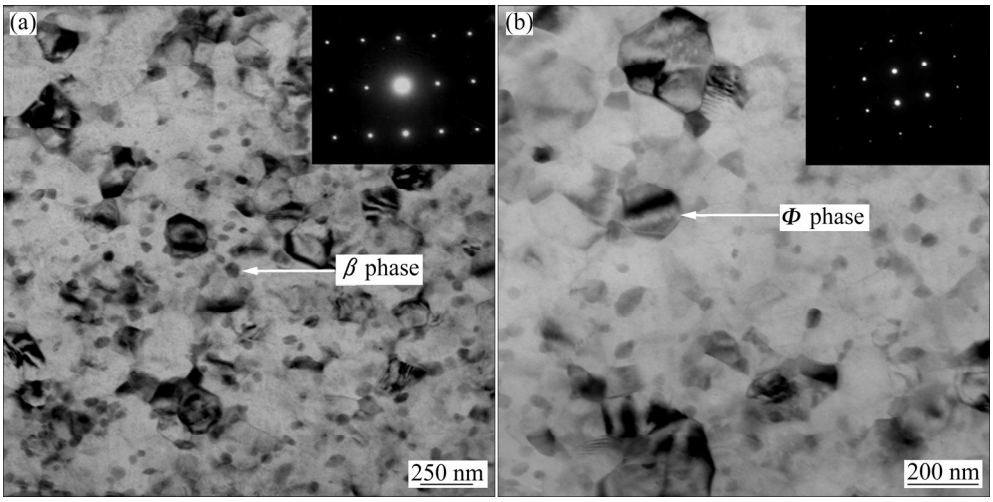

Fig. 8 TEM images of AM50−4%(Zn,Y) alloy treated at 180 °C for 12 h ($T6_{II}$): (a) β phase; (b) Φ phase

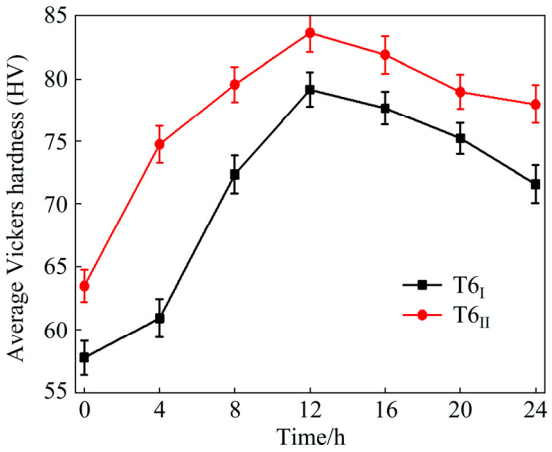

Fig. 9 Age-hardening curves of AM50−4%(Zn,Y) alloys treated at 180 °C for different time ($T6_I$ and $T6_{II}$)

3.5 Tensile properties

The tensile stress−strain curves of the AM50−4%(Zn,Y) alloy with as-cast, solid-solution and peak-aging states are shown in Fig. 10. Table 2 lists the typical tensile properties of the alloys in different states. The two-step progressive heat treatment obviously enhanced the age-strengthening effect on improving tensile properties of the alloy more than the one-step heat treatment. The tensile strength of the alloys was improved significantly after the aging treatment. The $T6_{II}$ heat-treated alloy possessed optimal tensile properties; the values of UTS, YS and δ were 231 MPa, 126 MPa and 8.5%, respectively.

The solid solution strengthening was not significant due to the weakened second-phase strengthening that

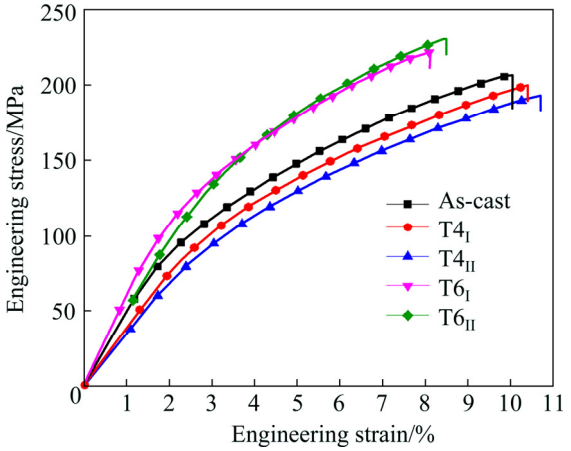

Fig. 10 Tensile stress−strain curves of AM50−4%(Zn,Y) alloy with different states

Table 2 Tensile properties of AM50−4%(Zn,Y) alloy with different states

State	UTS/MPa	YS/MPa	δ/%
As-cast	207	93	10.0
$T4_I$ (345 °C, 16 h)	198	86	10.4
$T4_{II}$ (345 °C, 16 h)+(375 °C, 6 h)	193	83	10.7
$T6_I$ (180 °C, 12 h)	222	109	8.1
$T6_{II}$ (180 °C, 12 h)	231	126	8.5

would deteriorate the strength of the alloy. Because of this, the UTS and YS values decreased slightly after the solution treatment. According to previous research, the interdendritic intermetallics are prone to split up due to stress concentration during the loading process, which in turn causes the brittle intergranular cracks [19]. The notable improvement of the strength was mainly ascribed to the dissolved second phase and supersaturation degree of α-Mg as a result of the subsequent aging treatment. However, in the present study, the ductility decreased slightly. As for the aged Mg−Al−Zn system alloys, the fine continuous precipitates throughout the α-Mg grain were more beneficial for improving the strength of the alloys [20,21]. For the $T6_I$ heat-treated alloy, the strength of the alloy increased remarkably. This was attributed to the amount of fine precipitates which had formed in the matrix, and which were distributed around the grain boundaries after the aging treatment. On the other hand, the unsolved β-phase was still distributed at the grain boundaries and the matrix, which resulted in deteriorating the ductility of the alloy. Compared to $T6_I$ heat-treated alloy, more fine precipitates were formed in the $T6_{II}$ heat-treated alloy during the subsequent aging process. This can be attributed to the fact that most of the Φ and β phases dissolved into the α-Mg matrix by the two-step progressive solution treatment. The fine continuous precipitates that dispersed uniformly throughout the grains could effectively hinder the dislocation movement, leading to a distinct precipitation strengthening effect.

4 Conclusions

1) The AM50−4%(Zn,Y) alloy was mainly composed of the α-Mg matrix, the β-$Mg_{17}(Zn,Al)_{12}$ phase and the lamellar Φ-$Mg_{21}(Zn,Al)_{17}$ phase. Additionally, some amounts of granular Al_6YMn_6 and Al_2Y phases were found in the alloy.

2) With the addition of Zn, the formation temperature of the β phase, which is formed by the eutectic reaction of $L\rightarrow\alpha$-Mg+β, decreased from 437 to 382.3 °C. The Φ-phase was formed by the peritectic reaction of $L+\beta\rightarrow\Phi+\alpha$-Mg at 353.8 °C.

3) A two-step progressive solution treatment could make the Φ and β phases sufficiently dissolve into the matrix, which resulted in the formation of fine precipitates in the subsequent following aging process.

4) The two-step progressive heat treatment had a more obviously enhanced age-strengthening effect on improving the mechanical properties of AM50−4%(Zn,Y) alloy than that of the one-step heat treatment. After the $T6_{II}$ treatment ((345 °C, 16 h + 375 °C, 6 h) + (180 °C, 12 h)), the values of UTS, YS and δ of the alloy were 231 MPa, 126 MPa and 8.5%, respectively.

References

[1] AGNEW S R, NIE J F. Preface to the viewpoint set on: The current state of magnesium alloy science and technology[J]. Scripta Materialia, 2010, 63(7): 671−673.

[2] ZHAO Chao-yong, PAN Fu-sheng, PAN Hu-cheng. Microstructure, mechanical and bio-corrosion properties of as-extruded Mg−Sn−Ca alloys [J]. Transactions of Nonferrous Metals Society of China, 2016, 26(6): 1574−1582.

[3] KUMAR P, MONDAL A K, CHOWDHURY S G, KRISHNA G, RAY A K. Influence of additions of Sb and/or Sr on microstructure and tensile creep behaviour of squeeze-cast AZ91D Mg alloy [J]. Materials Science and Engineering A, 2017, 683: 37−45.

[4] ZHANG Su-qing, CHEN Ti-jun, CHENG Fa-liang, LI Lei-liang. Microstructural evolution and phase transformation during partial remelting of in-situ Mg_2Si_p/AM60B composite [J]. Transactions of Nonferrous Metals Society of China, 2016, 26(6): 1564−1573.

[5] KIM J M, PARK J S, KIM K T. Influence of Sn content on the mechanical and corrosion behavior of AM60 base alloys [J]. Advanced Materials Research, 2012, 378−379: 697−700.

[6] ZHU S M, ABBOTT T B, GIBSON M A, NIE J F, EASTON M A. Age hardening in die-cast Mg−Al−RE alloys due to minor Mn additions [J]. Materials Science and Engineering A, 2016, 656: 34−38.

[7] ZHANG Jing, GUO Z X, PAN Fu-sheng, LI Zhong-sheng, LUO Xiao-dong. Effect of composition on the microstructure and mechanical properties of Mg−Zn−Al alloys [J]. Materials Science and Engineering A, 2007, 456(1−2): 43−51.

[8] ZHU Shao-zhen, LUO Tian-jiao, ZHANG Ting-an, LI Ying-ju,

YANG Yuan-sheng. Effects of Cu addition on the microstructure and mechanical properties of as-cast and heat treated Mg−6Zn−4Al magnesium alloy[J]. Materials Science and Engineering A, 2017, 689: 203−211.

[9] DONG Xu-guang, FU Jun-wei, WANG Jing, YANG Yuan-sheng. Microstructure and tensile properties of as-cast and as-aged Mg−6Al−4Zn alloys with Sn addition [J]. Materials & Design, 2013, 51: 567−574.

[10] XIAO Wen-long, SHEN Yu-sen, WANG Li-dong, WU Yao-ming, CAO Zhan-yi, JIA Shu-sheng, WANG Li-min. The influences of rare earth content on the microstructure and mechanical properties of Mg−7Zn−5Al alloy [J]. Materials & Design, 2010, 31(7): 3542−3549.

[11] LIANG Song-mao, MA Yue-qun, CHEN Rong-shi, HAN En-hou. Optimization of heat treatment in AZ64 magnesium alloy [J]. Materials transactions, 2008, 49(5): 986−989.

[12] WANG Feng, MA De-zhi, WANG Zhi, MAO Ping-li, LIU Zheng. Microstructure, mechanical properties and solidification behavior of AM50−*x* (Zn, Y) magnesium alloys [J]. Acta Metallurgica Sinica, 2016, 52(9): 1115−1122. (in Chinese)

[13] WANG Jian-li, PENG Qiu-ming, WU Yao-ming, WANG Li-min. Microstructure and mechanical properties of Mg−6Al−4RE−0.4Mn alloy [J]. Transactions of Nonferrous Metals Society of China, 2006, 16(S1): s703−s707.

[14] ZHAO Zu-de, CHEN Qiang, WANG Yan-bin, SHU Da-yu. Microstructures and mechanical properties of AZ91D alloys with Y addition [J]. Materials Science and Engineering A, 2009, 515(1−2): 152−161.

[15] HOU Dan-hui, LIANG Song-mao, CHEN Rong-shi, DONG Chuang, HAN En-hou. Effects of Sb content on solidification pathways and grain size of AZ91 magnesium alloy [J]. Acta Metallurgica Sinica (English Letters), 2015, 28(1):115−121.

[16] WANG Ye-shuang, WANG Qu-dong, MA Chun-jiang, DING Wen-jiang, ZHU Yan-ping. Effects of Zn and RE additions on the solidification behavior of Mg−9Al magnesium alloy [J]. Materials Science and Engineering A, 2003, 342(1−2): 178−182.

[17] HOU Dan-hui, LIANG Song-mao, CHEN Rong-shi, DONG Chuang. Solidification behavior and grain size of sand casting Mg−6Al−*x*Zn alloys [J]. Acta Metall Sinica, 2014, 50(5): 601−609. (in Chinese)

[18] OHNO M, MIRKOVIC D, SCHMID-FETZER R. Phase equilibria and solidification of Mg-rich Mg−Al−Zn alloys [J]. Materials Science and Engineering A, 2006, 421(1−2): 328−337.

[19] KIM B, DO J, LEE S, PARK I. In situ, fracture observation and fracture toughness analysis of squeeze cast AZ51−*x*Sn magnesium alloys [J]. Materials Science and Engineering A, 2010, 527(24−25): 6745−6757.

[20] CEIOTTO S. TEM study of continuous precipitation in Mg−9wt%Al−1wt%Zn alloy [J]. Acta Materialia, 2000, 48(8): 1775−1787.

[21] LAI Wei-jen, LI Yi-yun, HSU Yung-fu, TRONG Shan, WANG Wen-hsiung. Aging behaviour and precipitate morphologies in Mg−7.7Al−0.5Zn−0.3Mn (wt.%) alloy [J]. Journal of Alloys and Compounds, 2009, 476(1): 118−124.

AM50−4%(Zn, Y)合金两步递进固溶与时效处理增强强化

代 帅，王 峰，马德志，王 志，刘 正，毛萍莉

沈阳工业大学 材料科学与工程学院，沈阳 110870

摘 要：基于热分析结果，对 AM50−4%(Zn,Y)(Zn/Y 摩尔比为 6:1)合金设计并实施一种两步递进固溶处理。利用 OM、XRD、SEM/EDS、TEM、拉伸实验和硬度实验研究固溶与时效处理对 AM50−4%(Zn,Y)合金组织与力学性能的影响。结果表明：与一步固溶处理相比，两步递进固溶处理能够使 Φ 和 β 相充分溶解于基体，获得更高的溶质过饱和度，从而一定程度上增强合金在后续时效处理中的弥散强化效果。在 180 °C 进行时效处理时，Φ 相析出对合金综合力学性能的影响要大于 β 相。经两步递进固溶处理(345 °C, 16 h + 375 °C, 6 h)的 AM50−4%(Zn,Y)合金在时效处理(180 °C, 12 h)后获得峰时效强度。

关键词：AM50−4%(Zn,Y)合金；热分析；固溶；时效处理；显微组织；强化机制

(Edited by Xiang-qun LI)